Theory of Plasma Electron Contribution to the Electron-Beam–Excited Nitrogen Laser*

D. A. McArthur and J. W. Poukey
Sandia Laboratories, Albuquerque, New Mexico 87115
(Received 31 August 1973)

We describe a new and experimentally verified model of gas laser excitation by relativistic electron beams. It is shown that in the pressure range 1–50 Torr N_2, nearly all the excitation of the 3371-Å nitrogen laser is caused by low-energy plasma electrons (and *not* by primary or cascade electrons).

Intense relativistic electron beams are currently being used to pump various high-pressure gas lasers (e.g., N_2, H_2, Xe, and HF),[1-3] because such beams can deposit large amounts of energy in a gas in $\lesssim 10^{-7}$ sec. Excitation of the gas molecules can proceed through collisions either with primary beam electrons, with cascade electrons produced in primary ionization events, or with plasma electrons drifting in the electric field created by the beam propagation process.[4] Estimates of laser excitation by primary electrons[5] and by cascade electrons[2] have been made for the Xe and N_2 lasers, respectively, but no theory of the contribution from plasma electrons has been made. We report here the first detailed model of laser excitation by plasma electrons created by a relativistic electron beam.[6] Applied to the case of the N_2 3371-Å laser, without adjustable parameters the model yields calculated peak laser powers and pulse widths which agree within $\lesssim 30\%$ with the measurements of Patterson.[7] As the radius of the beam drift tube is increased, the model predicts higher laser power and a different pressure dependence, trends which agree with experiment[3,7] and are not predicted by the cascade electron model of Ref. 2.

The nitrogen laser represents a good test of the importance of excitation via plasma electrons, because such excitation takes place by electron exchange, which is not very probable for high-velocity primary electrons. As the primary electron pulse propagates down the laser tube, the rapidly changing current produces a longitudinal electric field E_z. The primary electrons also ionize some gas molecules, producing a few secondary electrons which then drift in the field E_z and avalanche to produce a plasma of electron density n_s. At the pressures considered here the number density N_g of neutral gas molecules is relatively high, and the plasma (even during the avalanche process) is dominated by electron–neutral-molecule collisions.[4] The plasma can then be regarded as a fluid with an average drift velocity w and a distribution function $f(\epsilon)$ which are functions only of E_z/N_g (here ϵ is the electron energy). The net-current model,[4] together with measurements of the beam radial shape, velocity, and loss rate in propagation,[7] yield n_s and E_z/N_g as functions of space and time along the laser tube.

The volume rate X at which plasma electrons excite ground-state molecules to an excited state having cross section $\sigma(\epsilon)$ is given by $X = n_s N_g \langle \sigma v \rangle$, where the angular brackets indicate an average over $f(\epsilon)$, and v is the velocity of a plasma electron of energy ϵ. Alternatively, regarding the plasma as an electron fluid, the number of electrons passing through an area ΔA in time dt is given by $n_s w\, \Delta A\, dt$, and X can be written $X = n_s w \times \Delta A\, dt\, \delta\, dx/\Delta A\, dx\, dt = n_s w \delta$, where δ is the prob-

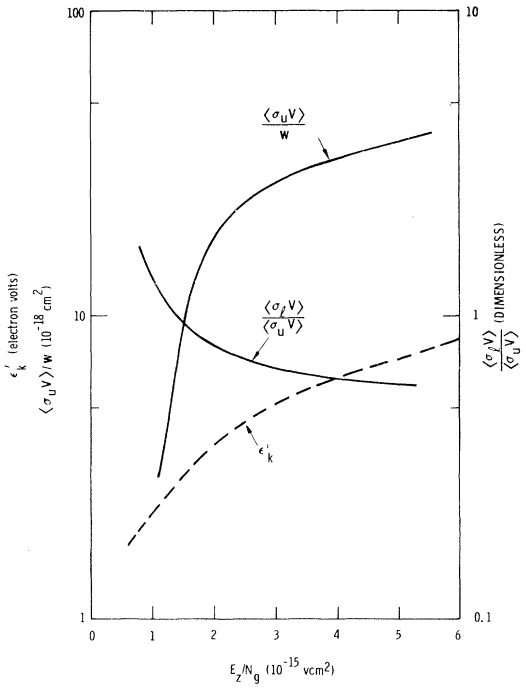

FIG. 1. Functions used for $\langle \sigma_u v \rangle$, $\langle \sigma_i v \rangle$, and ϵ_k', as functions of E_z/N_g.

ability per unit electron path length that an electron excites a molecule to the state of interest.[8] The upper (u) and lower (l) laser levels are the zero vibrational levels of the $C\,^3\Pi_u$ and $B\,^3\Pi_g$ electronic states, respectively. For the upper level we use experimentally measured data for $\langle\sigma_u v\rangle$: $X_u = 0.53 n_s w \delta_0$, where the coefficient $\delta_0/N_g = \langle\sigma_C v\rangle/w$ has been measured by Legler,[8] and 0.53 is a correction factor to remove contributions from $C\,^3\Pi_u$ levels higher than the zeroth (see Fig. 1). Since $\langle\sigma_l v\rangle$ is difficult to measure, we use $X_l = X_u\langle\sigma_l v\rangle/\langle\sigma_u v\rangle$, where we calculate as a function of E_z/N_g the ratio

$$\frac{\langle\sigma_l v\rangle}{\langle\sigma_u v\rangle} \cong \frac{\int_{\epsilon_l}^{\infty} \sigma_l \epsilon \exp(-\epsilon/\epsilon_k')\, d\epsilon}{\int_{\epsilon_u} \sigma_u \epsilon \exp(-\epsilon/\epsilon_k')\, d\epsilon}.$$

ϵ_l and ϵ_u are threshold energies, σ_l and σ_u are measured excitation cross sections,[9] and ϵ_k' gives the calculated Maxwellian tail of $f(\epsilon)$ at high energies[10] (see Fig. 1). Since the use of ϵ_k' also reproduces the shape of δ_0 to about $\pm 15\%$, this approximation appears to be as accurate as other input data to the calculation.

Using these excitation rates the gain on each rotational line is calculated, including the effects of spontaneous emission, collisions with ground-state molecules, and transitions between the C and B states induced by plasma electrons.[8-11] We assume that the laser light propagates only in the $+z$ direction, parallel to the electron beam, and that the region near the anode remains unsaturated.[2,12] Laser energy extraction from a volume element is efficient only when the light intensity is well above the saturation intensity. We therefore assume that laser energy is extracted from a volume element only if the total small-signal gain G (integrated from the anode along the light path to the volume element) is $G \geq G_0 = \exp(13)$.[13] The laser power density on the Jth P-branch transition, P_J, is given by equations which assume that the laser transition is saturated:

$$P_J = \tfrac{1}{2}[(f_J X_u - f_{J+1} X_l) - \bar{g}(f_J X_u + f_{J+1} X_l)] - \tfrac{1}{2} N_J [g_u(\tau_u^{-1} + a)(1-\bar{g}) + 1.57 g_u b(1+D)(1+\bar{g}) - 4.8 g_l bD \exp(-h\nu/\epsilon_k)(1-\bar{g}) - g_l \tau_l^{-1}(1+\bar{g})], \quad (1)$$

$$(g_u + g_l)\dot{N}_J = (f_J X_u + f_{J+1} X_l) - N_J\{g_u[\tau_u^{-1} + a - 1.57 b(1+D)] + g_l[\tau_l^{-1} - 4.8 bD \exp(-h\nu/\epsilon_k)]\}. \quad (2)$$

These equations differ from those of earlier workers[14] by considering individual rotational levels and by using a measured $\langle\sigma_u v\rangle$ and measured molecular collisional deactivation rates. The physical significance of these equations is discussed more fully in Ref. 14. Here $a = D/\tau_{su}$ and $b = B_{00}/\tau_{su}$, g_u and g_l are the rotational degeneracies of the laser levels, $\bar{g} = (g_u - g_l)/(g_u + g_l)$, and N_J is the average population per degenerate rotational sublevel. f_J is a function giving a Boltzmann rotational population distribution, τ_{su} is the spontaneous lifetime of the upper laser level, τ_u and τ_l are upper and lower-level lifetimes including collisional quenching, and B_{00} and $h\nu$ are the respective relative transition probability and photon energy of the 3371-Å band. D is a function of n_s and the plasma characteristic energy ϵ_k,[10] which gives excitation and de-excitation by plasma electrons.[11] The factors 1.57 and 4.8 include transitions from other vibrational levels of the C and B states. Summing contributions from those parts of the laser tube that satisfy $G(J) \geq G_0$, phased in time by the velocity of light, yields the calculated laser power.

D is a small correction at the peak of the laser pulse for the n_s and ϵ_k of Ref. 7, but may be more important for other conditions. The results are also not sensitive to the precise value of G_0, except near threshold (at high and low pressures). Details of the laser pulse shape are sensitive to the measured primary beam current wave form, and at high pressures it is important to take account of primary beam loss; this loss can decrease P_J at the end of the laser tube by as much as a factor of 5 compared to that in the anode region.

The calculated laser pulse appears on the initial portion of the primary current pulse, as n_s builds up rapidly and ϵ_k is still high. The calculated and experimental pulse shapes are similar, having rise times slightly shorter than the fall times. The calculated delay between the beginning of the primary beam pulse and the beginning of the laser pulse agrees well with the measurements of Ref. 7. The curves of Fig. 2, which assume a gas temperature of 300°K, give the peak laser power P_L at the drift-tube end. P_L is a strong function of the pressure p, with a maximum occurring at pressure p_m: below p_m, E_z/N_g is roughly constant and $n_s w$ decreases slowly, but $n_s w N_g$ increases; above p_m, E_z/N_g decreases,

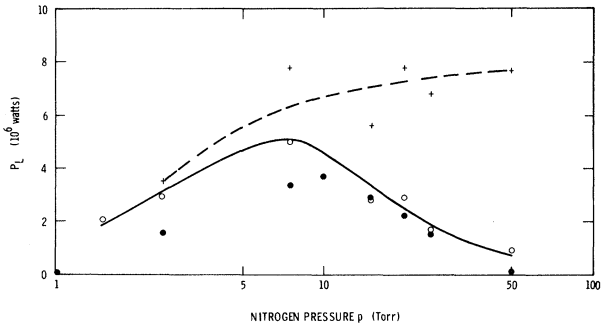

FIG. 2. Comparison of calculated and measured peak laser power as a function of nitrogen pressure. Filled circles, measurements of Ref. 7; open circles, calculations for the conditions of Ref. 7 ($r_0 = 2.5$ cm); crosses, calculations for the conditions of Ref. 7, except $r_0 = 5.0$ cm. Dashed and solid lines, smooth curves drawn through the calculated points.

resulting in lower $n_s w$ and P_L. $P_L(p_m)$ agrees with experiment within ~35%, the value of p_m agrees within ~25%, and the pressure width of the laser power curve agrees within ~20%. Over the pressure range from 2.5 to 25 Torr the average calculated laser pulse width (full width at half-maximum) is $\tau_L \cong 10$ nsec, agreeing with experiment within ~20%. These errors are within the uncertainties of X_u, X_l, and the measured parameters of the beam propagation.

The plasma current and ϵ_k vary considerably as one changes the drift-tube radius r_0,[4] so a check of the importance of plasma-electron excitation is the behavior of the calculated P_L as the drift-tube radius is changed. For a drift tube with radius $2r_0$ and unchanged primary beam propagation parameters, it can be seen in Fig. 2 that both p_m and $P_L(p_m)$ are larger than in the r_0 case, and τ_L increases by only 8%. The experiments of Ref. 3 used a drift tube of radius $\cong 2r_0$, and for a particular magnetic guide field both $P_L(p_m)$ and p_m itself were larger. Since the beam diameter, current, and drift-tube length in Ref. 3 are quite different from the conditions of Fig. 2, a quantitative comparison is not possible. However, Fig. 2 does show that the model displays the correct trends as the drift-tube diameter is changed.

The contribution of cascade electrons was estimated[9,15] to be $\lesssim 3\%$ of the plasma-electron contribution, even at 50 Torr. If neglected details of the lasing process were included in the model of Ref. 2 (such as the self-terminating laser action, existence of excitation to the lower level, lack of lasing on some rotational lines, and non-saturating laser intensity over part of the laser tube), their calculated laser energy would be reduced by about a factor of 20. We believe the resulting discrepancy would be removed by including the neglected process of plasma-electron excitation.

The model does not predict the absence of a second laser pulse following the primary beam pulse at the highest pressures (the calculated second laser pulse results from a rise in ϵ_k as the net current falls, and the collisional quenching of the lower laser level). However, the close agreement between the model presented here and the experimental P_L and τ_L, without the use of adjustable parameters, confirms the plasma electrons as an important (and perhaps dominant) excitation mechanism for some electron-beam–excited lasers. It is possible that low-energy plasma electrons also make important contributions to the high-energy HF chemical laser of Patterson and Gerber,[1] and to other lasers operating at sufficiently low pressures that a significant plasma current flows.

The authors gratefully acknowledge the cooperation of E. L. Patterson in making additional measurements to verify the theory, and acknowledge stimulating discussions with J. B. Gerardo.

*Work supported by the U.S. Atomic Energy Commission.

[1]R. T. Hodgson and R. W. Dreyfus, Phys. Rev. Lett. 28, 536 (1972); J. B. Gerardo and A. W. Johnson, IEEE J. Quantum Electron. 9, 748 (1973); E. L. Patterson and R. A. Gerber, to be published.

[2]R. W. Dreyfus and R. T. Hodgson, Appl. Phys. Lett. 20, 195 (1972).

[3]E. L. Patterson, J. B. Gerardo, and A. W. Johnson, Appl. Phys. Lett. 21, 293 (1972).

[4]D. A. McArthur and J. W. Poukey, Phys. Rev. Lett. 27, 1765 (1971); D. A. McArthur and J. W. Poukey, to be published.

[5]C. K. Rhodes, IEEE J. Quantum Electron. 9, 647 (1973).

[6]D. A. McArthur and J. W. Poukey, Bull. Amer. Phys. Soc. 17, 1032 (1972).

[7]E. L. Patterson, to be published.

[8]W. Legler, Z. Phys. 173, 169 (1963), Eqs. (1), (11), and (13).

[9]D. E. Shemansky and A. L. Broadfoot, J. Quant. Spectrosc. Radiat. Transfer 11, 1401 (1971).

[10]A. G. Engelhardt, A. V. Phelps, and C. G. Risk, Phys. Rev. 135, A1566 (1964).

[11]H. Van Regemorter, Astrophys. J. 136, 906 (1962), Eq. (22).

[12]R. W. Waynant, J. D. Shipman, Jr., R. C. Elton, and A. W. Ali, Appl. Phys. Lett. 17, 383 (1970).

[13]D. A. Leonard, Appl. Phys. Lett. 7, 4 (1965).
[14]E. T. Gerry, Appl. Phys. Lett. 7, 6 (1965); A. W. Ali, A. C. Kolb, and A. D. Anderson, Appl. Opt. 6, 2115 (1967), Eqs. (18) and (19).
[15]C. B. Opal, W. K. Peterson, and E. C. Beaty, J. Chem. Phys. 55, 4100 (1971).

Automodulation of an Intense Relativistic Electron Beam

M. Friedman
Naval Research Laboratory, Washington, D.C. 20375
(Received 23 October 1973)

A novel method of automodulating an intense relativistic electron beam has been demonstrated. The modulation is accomplished by passing the electron beam through a series of cavities that are inserted into a conventional drift tube. Experimental results indicate that the current is modulated at a frequency of 500 MHz at a relative modulation amplitude exceeding 80%.

Modulated electron beams have been the subject of many theoretical and experimental investigations. Their utility has been suggested or demonstrated for collective ion acceleration,[1,2] the production of hot plasmas,[3,4] and the generation of electromagnetic radiation.[5,6] Techniques for modulating low-power electron beams are relatively straightforward and are discussed in the literature.[7,8] In these techniques, external oscillating electric or magnetic fields are used to modulate the electron beam. The power in these oscillating fields must be of the same order of magnitude as the power in the electron beam. Thus, it is obvious that these techniques will be difficult to apply to a high-power relativistic electron beam.

A simple passive technique to modulate an intense relativistic electron beam of power greater than 10^{10} W is reported in this Letter. Beam-current modulation at a frequency of 500 MHz was achieved. The relative amplitude of the modulation apparently exceeded 80%. The experimental arrangement (Fig. 1) consisted of a foilless diode[9] emitting an annular electron beam with a current of ~15 kA and a voltage of ~500 kV for 50 nsec duration. The beam radius (at the diode) was 1.9 cm and its thickness was 0.2 cm. An

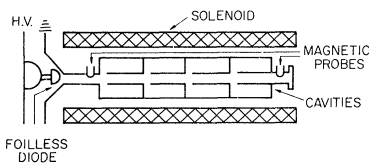

FIG. 1. Schematic of the experiment.

8-kG magnetic field confined the electron beam. The drift chamber consisted of a 1.2-m-long, 4.7-cm-i.d. stainless-steel tube. Four gaps feeding four coaxial cavities were inserted in the drift tube at various axial positions, as shown in Fig. 1. The length of each cavity was 15 cm and its outer diameter was 18 cm. The base pressure in the drift chamber and cavities was $\leq 10^{-5}$ Torr of air.

Several diagnostics were used to analyze the electron beam. Two magnetic probes, which measured the azimuthal component of the self magnetic field of the beam, were used to determine the rate of change of the beam current. These probes were located on either end of the multiple cavity structure. In addition, a Faraday cup was used to monitor beam current. Aluminum foils of different thickness were placed in front of the Faraday cup in order to estimate the mean electron kinetic energy from the attenuation of the measured beam current. Stray inductance in the Faraday cup (of the order of 10^{-10} H) limited the frequency response of the probe to ~100 MHz. In order to observe the current modulation directly, a small fast Faraday cup was used in which only a small portion of the beam was detected. The frequency response of this probe was greater than 1 GHz.

Figure 2 shows the beam voltage and Faraday-cup and fast-Faraday-cup signals. From the fast Faraday-cup signal one can see the current modulation of the electron beam. This probe samples parts of the beam passing through four holes located at different azimuthal and radial positions. The fast Faraday cup was connected through an ~20-m-long RGU-58 cable to a traveling-wave